Multi-point Conjugate Observations of Dayside ULF Waves during an Extended Period of Radial IMF

X. Shi[1,2], M. D. Hartinger[3,1], J. B. H. Baker[1], J. M. Ruohoniemi[1], D. Lin[2], Z. Xu[1], S. Coyle[1], B. S. R. Kunduri[1], L. M. Kilcommons[4], and A. Willer[5]

[1]Department of Electrical and Computer Engineering, Virginia Tech, Blacksburg, VA, USA.
[2]High Altitude Observatory, National Center for Atmospheric Research, Boulder, CO, USA.
[3]Space Science Institute, Boulder, CO, USA.
[4]Aerospace Engineering Sciences, University of Colorado Boulder, Boulder, Colorado, USA.
[5]National Space Institute at the Technical University of Denmark, Kgs. Lyngby, Denmark.

Key Points:

- Pc5 ULF waves were observed across the whole dayside from L∼5.5 into the polar cap region, in contrast to typical conditions
- Coordinated space and ground observations indicate that the waves on closed field lines were due to fundamental field line resonances
- The ion foreshock during radial IMF conditions provides seed perturbations for the growth of KH waves which generate the dayside ULF waves

Corresponding author: Xueling Shi, xueling7@vt.edu

Abstract

Long-lasting Pc5 ultralow frequency (ULF) waves spanning the dayside and extending from L∼5.5 into the polar cap region were observed by conjugate ground magnetometers. Observations from MMS satellites in the magnetosphere and magnetometers on the ground confirmed that the ULF waves on closed field lines were due to fundamental toroidal field line resonances (FLRs). Monochromatic waves at lower latitudes tended to maximize their power away from noon in both the morning and afternoon sectors, while more broadband waves at higher latitudes tended to have a wave power maximum near noon. The wave power distribution and anti-sunward wave propagation suggest surface waves on a Kelvin-Helmholtz (KH) unstable magnetopause coupled with FLRs. Based on satellite observations in the foreshock/magnetosheath, the more turbulent ion foreshock during an extended period of radial interplanetary magnetic field (IMF) likely plays an important role in providing seed perturbations for the growth of the KH waves.

Plain Language Summary

The Earth's magnetic field lines can oscillate at ultralow frequencies (ULF: 1 mHz - 5 Hz). These natural oscillations of closed magnetic field lines, analogous to vibrations on a stretched string, are also called geomagnetic pulsations or ULF waves. ULF waves play a key role in the transfer of energy from terrestrial space to Earth's upper atmosphere. In this study, we report a long-lasting large spatial scale ULF wave event observed by ground observatories from both hemispheres. Together with satellite measurements in space, we are able to confirm that these waves were driven by upstream turbulent structures due to the interaction between matter and electromagnetic fields emitted from the Sun and the Earth's outer atmosphere and magnetic field.

1 Introduction

Ultralow frequency (ULF; 1 mHz - 5 Hz) waves were identified as micropulsations or geomagnetic pulsations on the ground over fifty years ago (e.g. Jacobs et al., 1964). Since then, they have been recognized to play an important role in magnetospheric plasma energization/loss and energy transfer from the solar wind to Earth's magnetosphere and ionosphere (Elkington et al., 1999; Mathie & Mann, 2000; Rae et al., 2008). For example, they modulate ionospheric parameters (Pilipenko, Belakhovsky, Kozlovsky, et al., 2014), affect GPS (Karatay et al., 2010; Pilipenko, Belakhovsky, Murr, et al., 2014), and cause ionospheric heating (Crowley et al., 1985; Dessler, 1959). On the one hand, ULF waves driven by external sources from the solar wind can accelerate particles in the ring current and radiation belts through drift-bounce resonance (Zong et al., 2017). On the other hand, they can be driven by unstable particle distributions in the magnetosphere (e.g. Baddeley et al., 2005; Shi et al., 2018), and dissipate their energy to the ionosphere via Joule heating through field line resonances (FLRs) (Rae et al., 2008; Hartinger et al., 2011). When propagating to the ground, ULF waves provide a useful diagnostic probe of several magnetospheric properties (Menk et al., 1999) and can potentially drive geomagnetically induced currents (GIC) that may damage technological infrastructures (Pulkkinen & Kataoka, 2006; Pulkkinen et al., 2017). The spatial variation of the frequency and amplitude of geomagnetic perturbations is particularly important for predicting GIC and radiation belt dynamics and for remote sensing magnetospheric parameters.

The excitation of toroidal Pc5 waves is mainly due to external sources, i.e., an energy source in the solar wind, magnetosheath, or magnetopause/boundary layer. Coherent oscillations in solar wind parameters can penetrate and directly drive ULF waves inside the magnetosphere (Kepko & Spence, 2003). ULF waves can also be generated by buffeting of the magnetosphere in response to solar wind pressure perturbations, such as positive or negative dynamic pressure pulses (X. Y. Zhang et al., 2010). Surface waves that are unstable to the Kelvin-Helmholtz (KH) instability on the flanks of the magne-

tosphere are another external source for ULF wave generation (Miura, 1992). Surface waves can set up global waveguide modes and both surface waves and waveguide modes can couple to standing shear Alfvén waves through mode conversion (Rae et al., 2005). These shear Alfvén waves are often referred to as field line resonances (FLRs). In this study, we will not differentiate between resonant and non-resonant mode conversion.

Upstream waves originating from the ion foreshock have long been thought to drive dayside Pc3-4 pulsations (Takahashi et al., 1984; Yumoto et al., 1985), which is favored under predominately radial interplanetary magnetic field (IMF) or low cone angle conditions (Russell et al., 1983; Bier et al., 2014). More recent observations have shown that foreshock disturbances, such as hot flow anomalies, can also drive compressional Pc5 waves and FLRs in the dayside magnetosphere and ionosphere with significant amplitude (Hartinger et al., 2013; Shen et al., 2018; Wang et al., 2018). Hybrid simulations have also shown that high-speed jets and low frequency waves can form downstream of the quasi-parallel shock in the magnetosheath (Omidi et al., 2014; Palmroth et al., 2015, 2018); these foreshock associated disturbances and ULF waves can act as seed fluctuations for the generation of KH waves on the magnetopause (Miura, 1992).

In this letter, we report long-lasting Pc5 waves with an unusually large spatial extent (from L∼5.5 to the polar cap region on the dayside) observed by conjugate ground magnetometers during an extended period of radial IMF condition on Jan 25, 2016; on closed field lines, these correspond to the fundamental toroidal mode. We argue that these waves are due to magnetopause surface waves caused by a KH-unstable magnetopause seeded by foreshock transients.

2 Observations

2.1 Event Overview

Figure 1 provides an overview of the interplanetary and geomagnetic conditions during the event and maps showing locations of ground magnetometers and footprints of other measurements from satellites. The interplanetary parameters (Figure 1a-c) are obtained from the WIND satellite, time shifted by 45 minutes. As shown in Figure 1a-b, the IMF is dominated by the B_x component (red curve) which leads to a low cone angle condition and very quiet geomagnetic activity throughout the day (Figure 1d). No obvious periodic or abrupt perturbations were observed in the solar wind velocity or dynamic pressure (Figure 1c). However, large spatial-scale long-lasting ULF waves were observed by two conjugate latitudinal ground magnetometer chains (Figure 1e). Black traces indicate measurements from geomagnetic stations along the west coast of Greenland operated by the Technical University of Denmark (DTU). Red traces indicate measurements from the Autonomous Adaptive Low Power Instrument Platform (AAL-PIP) ground magnetometer chain located on the 40° magnetic meridian between the 80°-85° South geographic latitude, 70°-79° magnetic latitude (Clauer et al., 2014). Note that the time resolution from both ground magnetometer chains is 1 s except for the ATU station which is 10 s. (There were data quality issues with the ATU station on this date, so we only show its time series in Figure 1e and exclude it from further analysis in the following sections.)

The auroral image obtained from the Special Sensor Ultraviolet Spectrographic Imager (SSUSI) on board the Defense Meteorological Satellite Program (DMSP) satellite shows that ULF waves were observed on both closed and open magnetic field lines (Figure 1f). Black (red) stars indicate locations of the DTU (AAL-PIP) stations. The AAL-PIP stations (PG1-5) were mapped from the southern hemisphere using the T96 external model and IGRF08 internal model. PG0 appears to be on T96 open field lines and so cannot be mapped to the northern hemisphere. SSJ measurements from DMSP (Figure S1) also indicate that THL was in the polar cap region and that soft electron pre-

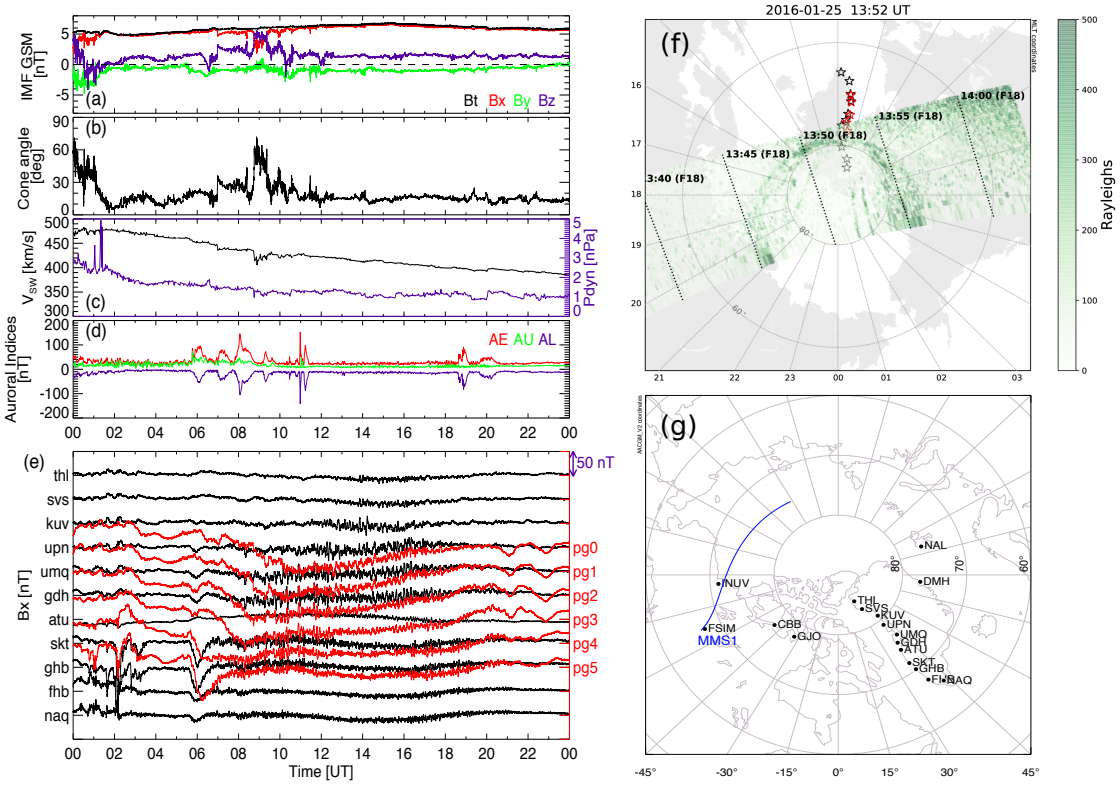

Figure 1. Event overview: (a) IMF components in GSM coordinates; (b) IMF cone angle; (c) solar wind velocity (black) and dynamic pressure (purple); (d) auroral indices; (e) time series of northward magnetic field component (B_x) in conjugate ground magnetometer observations from the DTU (black lines) stations in the northern hemisphere and the AAL-PIP (red lines) stations in the southern hemisphere; maps showing (f) DMSP SSUSI image (green pixels), locations of the DTU (black star) and AAL-PIP (red star, mapped from the southern hemisphere using the T96 external model and IGRF08 internal model) stations in magnetic local time coordinates and (g) footprint of MMS1 (blue curve) from 15 to 23 UT on Jan 25, 2016 and selected ground magnetometer locations (black dot) in AACGM coordinates.

cipitation was observed above it (Kilcommons et al., 2017). Figure 1g shows footprints of the MMS1 satellite from 15 to 23 UT on Jan, 25, 2016 and the locations of ground magnetometers in the northern hemisphere, including one latitudinal chain (DTU) and one longitudinal chain from which data will be analyzed in section 2.2 (Figure 2) and the FSIM and INUV stations from which data will be analyzed in section 2.3 (Figure 4).

On the same day, long-lasting second harmonic poloidal Pc4 waves were observed in the dayside magnetosphere and ionosphere by two GOES satellites and three SuperDARN radars located at high latitudes (Shi et al., 2018). As these waves had high-m numbers, they were screened by the ionosphere and thus not observed by the ground magnetometers.

2.2 Observations from the Ground

In this section we present wave properties from ground magnetometer observations in both hemispheres. Figure 2 shows dynamic power spectra of magnetic field data from the two latitudinal (upper panels) and longitudinal (lower panels) chains in the northern hemisphere. The spectra were obtained by applying a 60 min running Fast Fourier Transform (FFT) and incrementing by 15 min so that the evolution of the wave power can be obtained. Prior to taking the FFT, the data were detrended by subtracting a 30 min running average and a Hanning window was applied to reduce spectral leakage.

The panels in Figure 2a-b show the wave spectral power variation with latitude from the DTU chain. Noon is denoted by the second vertical line. Pc5 pulsations were mainly observed on the dayside with wave peak power frequency (black solid curve) slightly increasing with decreasing latitude (from top to bottom). It can be seen that the frequency stays fairly constant at all local times on the dayside. Wave power from lower latitudes (more monochromatic waves) tends to maximize away from noon in the morning/afternoon sector, while wave power from higher latitudes (more broadband waves) tends to maximize near noon. Comparing Figure 2a (B_x) with Figure 2b (B_y) reveals wave power in the morning sector is generally greater in the B_x component (toroidal mode, Figure 2a) than in the B_y component (poloidal mode, Figure 2b). However, the wave power is comparable for both components in the afternoon sector.

The panels in Figure 2c-d show the wave spectral power variation with local time from the longitudinal chain (see Figure 1g for locations). It can be clearly seen that ULF wave activity persisted across the whole dayside throughout the entire day. Five ground magnetometers located at similar magnetic latitudes but different magnetic longitudes started to pick up ULF wave activity around dawn (first vertical line on the left of the local noon annotation). The wave activity persisted toward local noon (vertical line indicated by the local noon annotation) and gradually disappeared in the late afternoon or dusk (vertical line on the right of the local noon annotation).

In Figure 3, we show time series and integrated wave power distribution for the Pc5 frequency range (1-7 mHz) from two conjugate chains, i.e., the DTU chain and the AAL-PIP chain. From the inter-hemispheric comparison of magnetic field time series (see Figure S2 for zoomed version), we can see that the H (B_x) component is mostly in phase between the hemispheres (Figure S2a) while the D (B_y) component is out of phase at the conjugate points (Figure S2b), which is consistent with odd mode FLR theory. The integrated wave power of the H component (Figure 3c) from higher (lower) latitudes tends to maximize (minimize) near noon. For the Pc5 toroidal component, the integrated wave power is generally stronger in the northern hemisphere (Figure 3c) than it is in the southern hemisphere (Figure 3e). The Pc5 wave power in the poloidal component (Figure 3d and 3f) dominates in the afternoon sector (after ∼14:00 UT) and is generally stronger in the southern hemisphere.

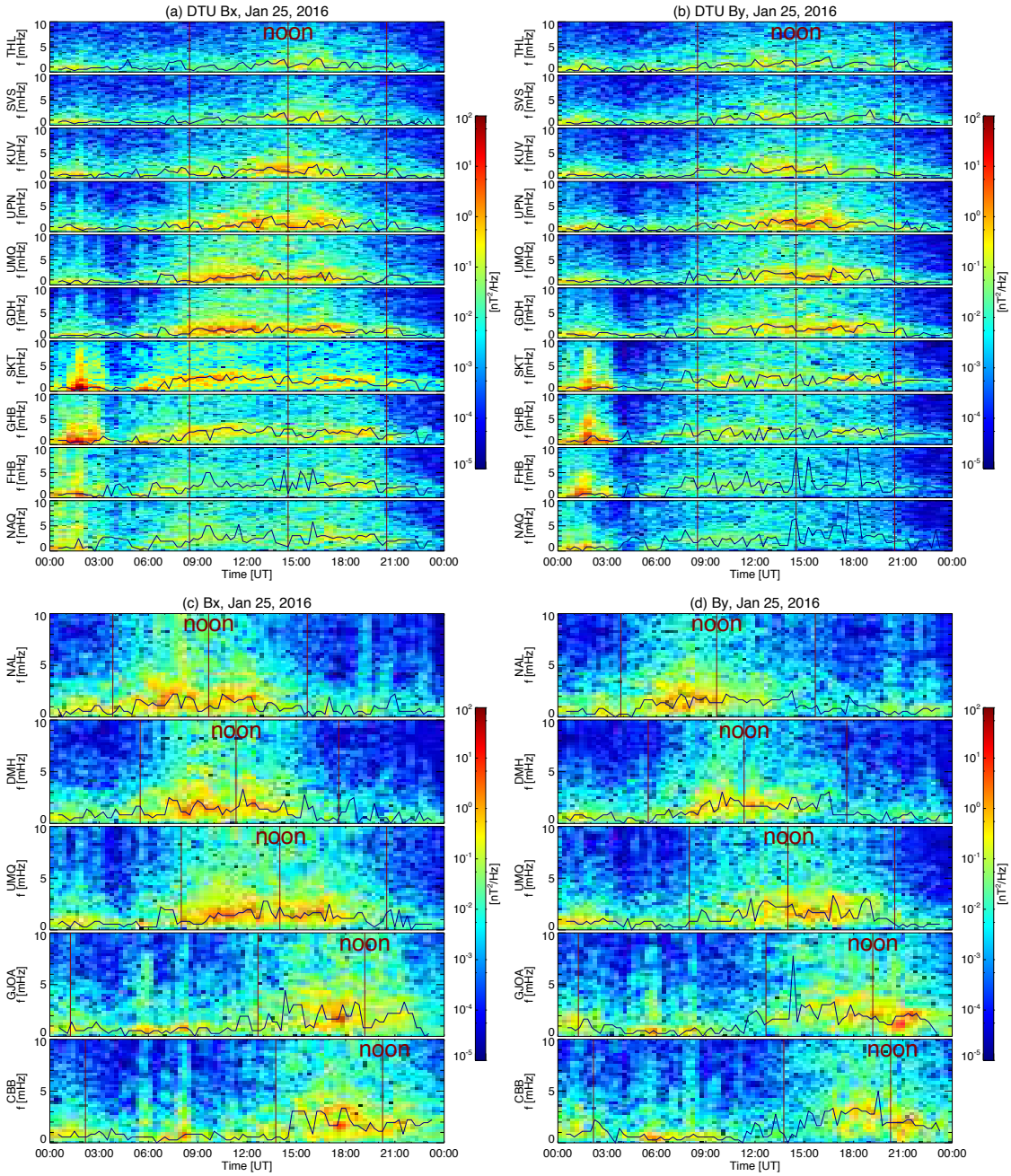

Figure 2. Dynamic power spectra of ground magnetic field (a) northward component (B_x) observed at the DTU stations; (b) eastward component (B_y) observed at the DTU stations; (c) northward component (B_x) observed at the longitudinal chain stations; (d) eastward component (B_y) observed at the longitudinal chain stations. Vertical lines indicate magnetic local times at 06 h, 12 h, and 18 h. Black solid traces identify the peak power frequency variation with time.

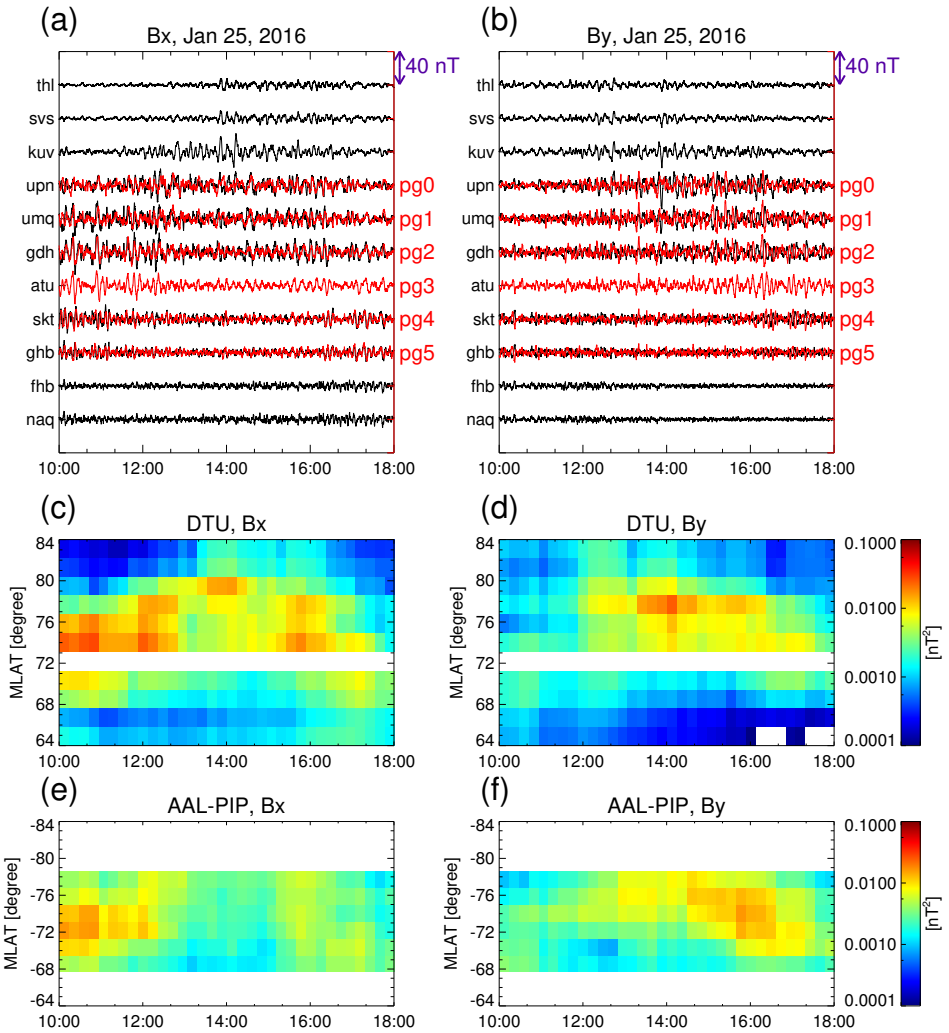

Figure 3. Inter-hemispheric comparison of ground magnetic field data from 10 to 18 UT on Jan 25, 2016 centered around local noon. Upper two panels show: (a) time series of B_x from the DTU (black) and AAL-PIP (red) stations; (b) time series of B_y from the DTU (black) and AAL-PIP (red) stations. Lower four panels show: variation of integrated wave power in the Pc5 frequency range with time and magnetic latitude for (c) DTU B_x, (d) DTU B_y, (e) AAL-PIP B_x, and (f) AAL-PIP B_y.

In addition to the Greenland stations, we checked the ULF wave signatures from lower L shells in the AUTUMNX stations (Connors et al., 2016) to see how far these waves can penetrate into the inner magnetosphere. Figure S3 shows that the Pc5 wave power becomes significantly weaker beyond the KJPK station (L∼5.5) and the wave power peaks at higher frequencies in the Pc3-4 frequency range at lower L shells (e.g., the VLDR station and others not shown). In addition to the ground magnetometers, the ground-based SuperDARN radars observed Pc5 ULF waves at other local times (Figure S4). As shown in Figure S4 (left) from the Inuvik radar, the waves extended deep into the polar cap. To summarize, ground magnetometers and SuperDARN radars indicate that Pc5 wave activity extended from L∼5.5 deep into the polar cap.

2.3 Observations from Space

We now analyze wave signatures in the magnetosphere from MMS satellite observations. Although the observation times of the MMS satellites were different from the DTU/AAL-PIP conjugate ground magnetometer observations, the solar wind conditions were similar during this interval and the footprint of the MMS1 satellite passed near two other ground magnetometer stations (FSIM and INUV) as shown in Figure 1g. Note that MMS1 crossed the magnetopause and moved into the magnetosheath at the end of this day. Figure 4a-b shows the IMF and dynamic pressure time series from the WIND satellite (45 minutes shifted) indicating upstream conditions. Monochromatic Pc5 waves were observed in the B_y component (the azimuthal component in the mean-field-aligned coordinates) measured by MMS1 at 17-19 UT (Figure 4c-d). Wave peak power frequency (black line in Figure 4d) and wave power gradually decreased as MMS1 moved outward to higher L shells. The waveform also becomes more irregular, similar to the DTU chain observations (Figure 2a and 3a). The other three MMS satellites observed similar wave activity (not shown). FSIM and INUV stations at fixed L shells observed Pc5 waves at similar frequencies throughout the 15-23 UT time interval. Wave power and peak power frequency gradually decreased after 21 UT as these stations moved towards local noon.

3 Discussion

ULF waves extending from L ∼5.5 into the polar cap region and across the whole dayside were observed by multiple ground magnetometers in both hemispheres on Jan 25, 2016. Perturbations in the toroidal component generally have larger power in the northern hemisphere than those in the southern hemisphere (Figure 3c and 3e). The toroidal component has stronger wave power in the morning sector compared to the afternoon sector (Figures 2a, 2c, 3c and 3e). For perturbations in the poloidal component, larger amplitudes were observed in the southern hemisphere afternoon sector (Figure 3d and 3f). It is unlikely that ionospheric conductivity could explain the north-south asymmetries seen at all magnetometer station pairs since the asymmetries in precipitation and solar radiation are different at different latitudes yet we see similar patterns at all station pairs.

These inter-hemispheric and dawn-dusk asymmetries can be interpreted in terms of the IMF conditions and possible driving sources. As shown in Figure 1a, the IMF was dominated by an extended period of positive B_x, with slightly positive B_z and negative B_y. Stronger toroidal mode wave power in the northern hemisphere can be explained by this IMF orientation. Namely, the radially IMF dominant configuration favors formation of an ion foreshock upstream of the magnetopause (Eastwood et al., 2005). When both B_x and B_z are positive, a quasi-parallel foreshock favors the northern hemisphere, leading to a more turbulent magnetosheath and elevated ULF disturbances in the northern hemisphere (Guglielmi et al., 2017; Hwang & Sibeck, 2016).

The dawn-dusk asymmetry of toroidal mode standing Alfvén waves has long been attributed to the dawn-dusk asymmetry of the Kelvin-Helmholtz instability, which is ex-

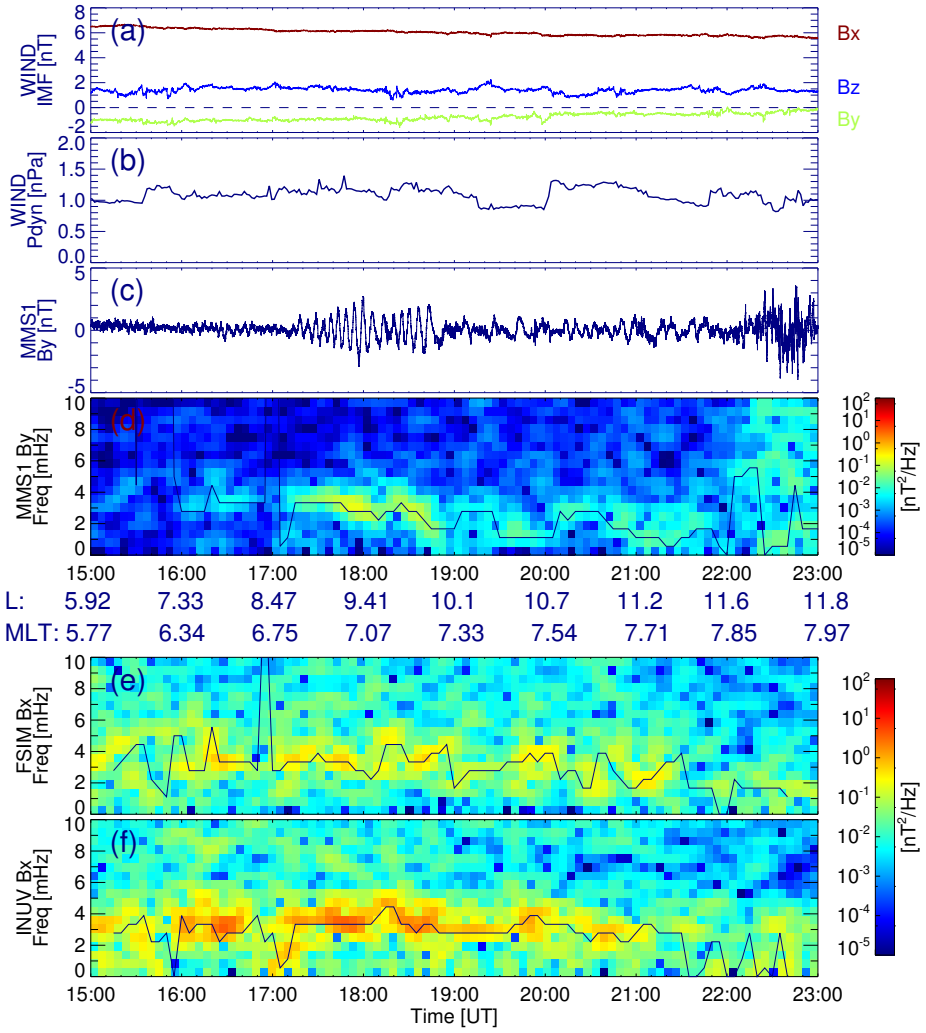

Figure 4. Coordinated observations of Pc5 waves from MMS1 and the FSIM an INUV ground magnetometers: (a) IMF components, (b) solar wind dynamic pressure, (c) MMS1 B_y time series, (d) MMS1 B_y dynamic power spectrum, (e) FSIM B_x dynamic power spectrum, and (f) INUV B_x dynamic power spectrum. Black solid traces in dynamic power spectra identify the peak power frequency variation with time.

pected from the asymmetry of the magnetosheath magnetic field that results from the IMF following the Parker spiral (Lee & Olson, 1980). At the same time, larger seed perturbations for the KH-instability would be expected at dawn during spiral IMF conditions that favor the formation of the ion foreshock pre-noon, further enhancing surface wave amplitudes at dawn. However, Takahashi et al. (2016) have shown that fundamental toroidal-mode standing Alfvén waves are stronger on the dawnside than on the duskside regardless of the orientation of the IMF due to the dawn-dusk asymmetry of the radial profile of the mass density, and the 3D simulation work by Wright et al. (2018) also showed that FLRs are excited with larger amplitude at dawn compared to dusk in an asymmetric magnetospheric waveguide system that is driven symmetrically about the noon meridian. It is possible that both external (IMF orientation) and internal (radial mass density variation) mechanisms described above were active in the dayside magnetosphere on Jan 25, 2016.

It is very unlikely that such large spatial scale and steady long-lasting ULF waves observed on the dayside were excited by instabilities internal to the magnetosphere (e.g. Shi et al., 2018), which usually excite poloidal mode waves with large azimuthal wavenumber that are difficult to detect with ground magnetometers (Hughes & Southwood, 1976). Thus we discuss the possibility of an external upstream source. We first exclude the solar wind direct driving source and solar wind pressure pulse driving source, since neither quasi-periodic solar number density/pressure or magnetic field variations at similar frequencies, nor large-amplitude, transient dynamic pressure pulses, were observed by the upstream WIND satellite (Figure 4a-b). One possible scenario is that the Pc5 waves observed on the dayside closed field lines are FLRs coupled to compressional ULF waves driven by surface waves at the KH-unstable magnetopause. We provide additional evidence for such a scenario:

1. The wave power distribution has a maximum around noon at higher latitudes and maxima in the morning/afternoon sector at lower latitudes (Figures 2a and 3c). The lower latitude peaks at dawn/dusk are consistent with surface waves coupling to FLRs, while the high-latitude peaks may be consistent with more direct observations of the seed perturbations for the surface waves (e.g., Guglielmi et al., 2017).
2. There is an anti-sunward wave propagation in the morning and afternoon sectors from SuperDARN radar observations (Figure S4 and text in the Supporting Information): azimuthal wave number (James et al., 2013) estimated from the Stokkseyri radar ($m \sim 1.5$, eastward at mlt $\sim$ 17 hours and mlat $\sim 72.5°$) and the Inuvik radar ($m \sim$ -1.7, westward at mlt $\sim$ 9 hours and mlat $\sim 79.4°$). This is consistent with a surface wave driver.
3. The steady northward IMF orientation (Figure 1a) possibly provides a persistent mechanism for KH wave generation (Lin et al., 2014; Kavosi & Raeder, 2015).
4. There are surface wave signatures from MMS1 observations of magnetopause oscillations from 03:30 to 03:45 UT (Figure S5).

Since radial IMF orientation dominated throughout this event, an ion foreshock formed upstream of the quasi-parallel bow shock introducing a broad range of perturbations such as the foreshock cavity and hot flow anomaly (Sibeck et al., 2002; H. Zhang et al., 2013). The more turbulent foreshock plays an important role in providing seed perturbations for the growth of KH waves (Miura, 1992; Nosé et al., 1995; Hwang & Sibeck, 2016). We also know that foreshock transients can drive magnetopause perturbations and ripples with corresponding ULF perturbations in the absence of a KH unstable magnetopause (Sibeck, 1990). The local time distribution with peak near noon at high latitudes is consistent with large foreshock disturbances seeding the growth of surface waves via KHI, but it would not be consistent with the classic KHI picture where small upstream seed perturbations drive the surface waves - in this case, there is almost no wave power at noon (e.g. Claudepierre et al., 2009, 2016).

An outstanding issue is how Pc5 waves are generated in the cusp and polar cap region on open field lines. The polar cap has generally been thought to be a quiet region, with wave power entering only from neighboring regions, such as the auroral oval (e.g. Bland & McDonald, 2016). As summarized in Engebretson et al. (2006) Pc5 waves from very high latitudes can be categorized into three classes according to their potential sources: cusp-related waves (Posch et al., 1999), polar pulsations extended from the auroral region, and $Pi_{cap}3$ independent of cusp and auroral pulsations (Yagova et al., 2004). For this particular event, it is possible the Pc5 waves on open field lines came directly from the magnetosheath and foreshock region, generating waves with very similar properties across a wide range of L, from deep in the polar cap to L∼5.5. Global ULF wave models taking into account kinetic processes in the foreshock region and magnetosheath are needed to reveal the exact driving mechanism of this new type of Pc5 event extending from L∼5.5 into the polar cap.

Finally, it should be emphasized that the waves observed in this study can potentially cause geospace impacts. This study shows that during radial IMF, foreshock transients/KHI can lead to the generation of spatially extended Pc5 wave activity. More work is needed to understand whether these types of waves have sufficient amplitude to generate significant dB/dt and GIC. Additionally, the multi-point conjugate observations in this study reveal that during radial IMF conditions, the properties of Pc5 ULF waves - frequency and amplitude - may vary little across a wide range of latitudes, in contrast to general expectations for standing Alfvén waves driven by external energy sources; this could have implications for predicting GIC (Pulkkinen et al., 2017) and radiation belt dynamics (Elkington, 2006).

4 Conclusions

Using conjugate inter-hemispheric observations we have examined the properties of ULF waves observed across the entire dayside during an extended period of radial IMF. The waves were observed from L ∼5.5 to the cusp and polar cap region with minimal frequency variations (1-4 mHz) over local time and latitude. Observations from MMS satellites and multiple inter-hemispheric ground magnetometers indicate that the Pc5 pulsations on closed field lines are fundamental toroidal mode FLRs. Wave power from lower latitudes (more monochromatic waves) tends to maximize away from noon in the morning/afternoon sector, while wave power from higher latitudes (more broadband waves) tends to maximize near noon. The wave power distribution and anti-sunward propagation suggest KH instability driven waves coupled with FLRs. The upstream ion foreshock may provide seed perturbations for the growth of the KH instability which generates the dayside Pc5 waves. No previous study has shown that global and steady Pc5 wave activity as reported in our study could be associated with B_x predominant conditions (or ion foreshock processes). This event is a good example of how low cone angle (and potentially ion foreshock processes) can be associated with Pc5 waves rather than only with Pc3-4 waves. Further investigations of this type of global and steady wave activity is needed to determine how often these driving conditions occur, to better assess how upstream foreshock/magnetosheath disturbances couple to magnetospheric ULF waves, and to determine whether these long-lasting Pc5 waves could cause geospace impacts such as GICs or radiation belt interactions.

Acknowledgments

The authors are grateful to Mary Hudson, Kazue Takahashi, Hui Zhang and Heli Hietala for helpful discussions and valuable comments. Work at Virginia Tech has been supported by National Aeronautics and Space Administration (NASA) Headquarters under the NASA Earth and Space Science Fellowship Program - Grant 80NSSC17K0456 P00001, National Science Foundation (NSF) grant AGS-1341918, and NASA 80NSSC19K0907. MDH, ZX, and SC were supported by NSF PLR-1543364 and PLR-1744828. DL was supported by

the Advanced Study Program Postdoctoral Fellowship of the National Center for Atmospheric Research (NCAR). NCAR is sponsored by the NSF. We acknowledge the use of DTU, AAL-PIP, and AUTUMNX ground magnetometer data. DTU data are obtained from the public Tromso Geophysical Observatory website (http://flux.phys.uit.no/geomag.html). The Antarctic AAL-PIP data have been provided by Virginia Tech which is supported by NSF through the following awards for this purpose: ANT0839858, ATM922979, ANT0838861, PLR-1243398, and PLR-1543364. AUTUMN/AUTUMNX groundbased magnetometer data are available at http://autumn.athabascau.ca/ website. We also wish to acknowledge the use of data from the MMS and WIND spacecraft. MMS data are available via MMS science data center (at https://lasp.colorado.edu/mms/sdc/public/). Solar wind data from the Wind spacecraft were obtained through the CDAWeb https://cdaweb.gsfc.nasa.gov/index.html/. We would like to thank Johns Hopkins University Applied Physics Laboratory for providing the DMSP/SSUSI auroral FUV data (available at https://ssusi.jhuapl.edu/data_products) and DMSP/SSJ data (available at https://www.ngdc.noaa.gov/stp/satellite/dmsp/). We also thank all participants in the worldwide SuperDARN collaboration for the distribution of SuperDARN data via the website (http://vt.superdarn.org/tiki-index.php?page=Data+Access).

References

Baddeley, L., Yeoman, T., Wright, D., Trattner, K., & Kellet, B. (2005). On the coupling between unstable magnetospheric particle populations and resonant high m ULF wave signatures in the ionosphere. *ANNALES GEOPHYSICAE*, *23*(2), 567-577. doi: {10.5194/angeo-23-567-2005}

Bier, E. A., Owusu, N., Engebretson, M. J., Posch, J. L., Lessard, M. R., & Pilipenko, V. A. (2014). Investigating the IMF cone angle control of Pc3-4 pulsations observed on the ground. *Journal of Geophysical Research: Space Physics*, *119*(3), 1797-1813. Retrieved from `https://agupubs.onlinelibrary.wiley.com/doi/abs/10.1002/2013JA019637` doi: 10.1002/2013JA019637

Bland, E. C., & McDonald, A. J. (2016). High spatial resolution radar observations of ultralow frequency waves in the southern polar cap. *Journal of Geophysical Research: Space Physics*, *121*(5), 4005–4016.

Claudepierre, S. G., Toffoletto, F. R., & Wiltberger, M. (2016). Global MHD modeling of resonant ULF waves: Simulations with and without a plasmasphere. *Journal of Geophysical Research: Space Physics*, *121*(1), 227-244. Retrieved from `https://agupubs.onlinelibrary.wiley.com/doi/abs/10.1002/2015JA022048` doi: 10.1002/2015JA022048

Claudepierre, S. G., Wiltberger, M., Elkington, S. R., Lotko, W., & Hudson, M. K. (2009). Magnetospheric cavity modes driven by solar wind dynamic pressure fluctuations. *Geophysical Research Letters*, *36*(13). Retrieved from `https://agupubs.onlinelibrary.wiley.com/doi/abs/10.1029/2009GL039045` doi: 10.1029/2009GL039045

Clauer, C., Kim, H., Deshpande, K., Xu, Z., Weimer, D., Musko, S., ... others (2014). An autonomous adaptive low-power instrument platform (AAL-PIP) for remote high-latitude geospace data collection. *Geoscientific Instrumentation, Methods and Data Systems*, *3*(2), 211.

Connors, M., Schofield, I., Reiter, K., Chi, P. J., Rowe, K. M., & Russell, C. T. (2016). The AUTUMNX magnetometer meridian chain in Québec, Canada. *Earth, Planets and Space*, *68*(1), 2.

Crowley, G., Wade, N., Waldock, J., Robinson, T., & Jones, T. (1985). High time-resolution observations of periodic frictional heating associated with a Pc5 micropulsation. *Nature*, *316*(6028), 528.

Dessler, A. (1959). Upper atmosphere density variations due to hydromagnetic heating. *Nature*, *184*(4682), 261.

Eastwood, J., Lucek, E., Mazelle, C., Meziane, K., Narita, Y., Pickett, J., & Treumann, R. (2005). The foreshock. *Space Science Reviews*, *118*(1-4),

41–94.

Elkington, S. R. (2006). A review of ULF interactions with radiation belt electrons. *GEOPHYSICAL MONOGRAPH-AMERICAN GEOPHYSICAL UNION*, *169*, 177.

Elkington, S. R., Hudson, M. K., & Chan, A. A. (1999). Acceleration of relativistic electrons via drift-resonant interaction with toroidal-mode Pc-5 ULF oscillations. *Geophysical Research Letters*, *26*(21), 3273-3276. Retrieved from https://agupubs.onlinelibrary.wiley.com/doi/abs/10.1029/1999GL003659 doi: 10.1029/1999GL003659

Engebretson, M., Posch, J., Pilipenko, V., & Chugunova, O. (2006). ULF waves at very high latitudes. *Geophysical monograph*, *169*, 137–156.

Guglielmi, A., Klain, B., & Potapov, A. (2017, Dec). North-south asymmetry of ultra-low-frequency oscillations of Earth's electromagnetic field. *Solar-Terrestrial Physics*, *3*(4), 26-31. doi: 10.12737/stp-34201703

Hartinger, M., Angelopoulos, V., Moldwin, M. B., Glassmeier, K.-H., & Nishimura, Y. (2011). Global energy transfer during a magnetospheric field line resonance. *Geophysical Research Letters*, *38*(12).

Hartinger, M., Turner, D., Plaschke, F., Angelopoulos, V., & Singer, H. (2013). The role of transient ion foreshock phenomena in driving Pc5 ULF wave activity. *Journal of Geophysical Research: Space Physics*, *118*(1), 299–312.

Hughes, W. J., & Southwood, D. J. (1976). The screening of micropulsation signals by the atmosphere and ionosphere. *Journal of Geophysical Research*, *81*(19), 3234-3240. Retrieved from https://agupubs.onlinelibrary.wiley.com/doi/abs/10.1029/JA081i019p03234 doi: 10.1029/JA081i019p03234

Hwang, K.-J., & Sibeck, D. G. (2016). Role of low-frequency boundary waves in the dynamics of the dayside magnetopause and the inner magnetosphere. In *Lowfrequency waves in space plasmas* (p. 213-239). American Geophysical Union (AGU). Retrieved from https://agupubs.onlinelibrary.wiley.com/doi/abs/10.1002/9781119055006.ch13 doi: 10.1002/9781119055006.ch13

Jacobs, J. A., Kato, Y., Matsushita, S., & Troitskaya, V. A. (1964). Classification of geomagnetic micropulsations. *Journal of Geophysical Research*, *69*(1), 180-181. Retrieved from https://agupubs.onlinelibrary.wiley.com/doi/abs/10.1029/JZ069i001p00180 doi: 10.1029/JZ069i001p00180

James, M. K., Yeoman, T. K., Mager, P. N., & Klimushkin, D. Y. (2013). The spatio-temporal characteristics of ULF waves driven by substorm injected particles. *Journal of Geophysical Research: Space Physics*, *118*(4), 1737-1749. Retrieved from https://agupubs.onlinelibrary.wiley.com/doi/abs/10.1002/jgra.50131 doi: 10.1002/jgra.50131

Karatay, S., Arikan, F., & Arikan, O. (2010). Investigation of total electron content variability due to seismic and geomagnetic disturbances in the ionosphere. *Radio Science*, *45*(05), 1–12.

Kavosi, S., & Raeder, J. (2015). Ubiquity of Kelvin–Helmholtz waves at Earths magnetopause. *Nature Communications*, *6*, 7019.

Kepko, L., & Spence, H. E. (2003). Observations of discrete, global magnetospheric oscillations directly driven by solar wind density variations. *Journal of Geophysical Research: Space Physics*, *108*(A6). Retrieved from https://agupubs.onlinelibrary.wiley.com/doi/abs/10.1029/2002JA009676 doi: 10.1029/2002JA009676

Kilcommons, L. M., Redmon, R. J., & Knipp, D. J. (2017). A new DMSP magnetometer and auroral boundary data set and estimates of field-aligned currents in dynamic auroral boundary coordinates. *Journal of Geophysical Research: Space Physics*, *122*(8), 9068-9079. Retrieved from https://agupubs.onlinelibrary.wiley.com/doi/abs/10.1002/2016JA023342 doi: 10.1002/2016JA023342

Lee, L. C., & Olson, J. V. (1980). Kelvin-helmholtz instability and the variation

of geomagnetic pulsation activity. *Geophysical Research Letters*, *7*(10), 777-780. Retrieved from https://agupubs.onlinelibrary.wiley.com/doi/abs/10.1029/GL007i010p00777 doi: 10.1029/GL007i010p00777

Lin, D., Wang, C., Li, W., Tang, B., Guo, X., & Peng, Z. (2014). Properties of Kelvin-Helmholtz waves at the magnetopause under northward interplanetary magnetic field: Statistical study. *Journal of Geophysical Research: Space Physics*, *119*(9), 7485-7494. Retrieved from https://agupubs.onlinelibrary.wiley.com/doi/abs/10.1002/2014JA020379 doi: 10.1002/2014JA020379

Mathie, R. A., & Mann, I. R. (2000). A correlation between extended intervals of ULF wave power and storm-time geosynchronous relativistic electron flux enhancements. *Geophysical Research Letters*, *27*(20), 3261-3264. Retrieved from https://agupubs.onlinelibrary.wiley.com/doi/abs/10.1029/2000GL003822 doi: 10.1029/2000GL003822

Menk, F., Orr, D., Clilverd, M., Smith, A., Waters, C., Milling, D., & Fraser, B. (1999). Monitoring spatial and temporal variations in the dayside plasmasphere using geomagnetic field line resonances. *Journal of Geophysical Research: Space Physics*, *104*(A9), 19955–19969.

Miura, A. (1992). Kelvin-Helmholtz instability at the magnetospheric boundary: Dependence on the magnetosheath sonic Mach number. *Journal of Geophysical Research: Space Physics*, *97*(A7), 10655-10675. Retrieved from https://agupubs.onlinelibrary.wiley.com/doi/abs/10.1029/92JA00791 doi: 10.1029/92JA00791

Nosé, M., Iyemori, T., Sugiura, M., & Slavin, J. A. (1995). A strong dawn/dusk asymmetry in Pc5 pulsation occurrence observed by the DE-1 satellite. *Geophysical Research Letters*, *22*(15), 2053-2056. Retrieved from https://agupubs.onlinelibrary.wiley.com/doi/abs/10.1029/95GL01794 doi: 10.1029/95GL01794

Omidi, N., Sibeck, D., Gutynska, O., & Trattner, K. J. (2014). Magnetosheath filamentary structures formed by ion acceleration at the quasi-parallel bow shock. *Journal of Geophysical Research: Space Physics*, *119*(4), 2593-2604. Retrieved from https://agupubs.onlinelibrary.wiley.com/doi/abs/10.1002/2013JA019587 doi: 10.1002/2013JA019587

Palmroth, M., Archer, M., Vainio, R., Hietala, H., Pfau-Kempf, Y., Hoilijoki, S., ... Eastwood, J. P. (2015). ULF foreshock under radial IMF: THEMIS observations and global kinetic simulation Vlasiator results compared. *Journal of Geophysical Research: Space Physics*, *120*(10), 8782-8798. Retrieved from https://agupubs.onlinelibrary.wiley.com/doi/abs/10.1002/2015JA021526 doi: 10.1002/2015JA021526

Palmroth, M., Hietala, H., Plaschke, F., Archer, M., Karlsson, T., Blanco-Cano, X., ... others (2018). Magnetosheath jet properties and evolution as determined by a global hybrid-vlasov simulation. In *Annales geophysicae.*

Pilipenko, V., Belakhovsky, V., Kozlovsky, A., Fedorov, E., & Kauristie, K. (2014). ULF wave modulation of the ionospheric parameters: Radar and magnetometer observations. *Journal of Atmospheric and Solar-Terrestrial Physics*, *108*, 68–76.

Pilipenko, V., Belakhovsky, V., Murr, D., Fedorov, E., & Engebretson, M. (2014). Modulation of total electron content by ULF Pc5 waves. *Journal of Geophysical Research: Space Physics*, *119*(6), 4358–4369.

Posch, J. L., Engebretson, M. J., Weatherwax, A. T., Detrick, D. L., Hughes, W. J., & Maclennan, C. G. (1999). Characteristics of broadband ULF magnetic pulsations at conjugate cusp latitude stations. *Journal of Geophysical Research: Space Physics*, *104*(A1), 311-331. Retrieved from https://agupubs.onlinelibrary.wiley.com/doi/abs/10.1029/98JA02722 doi: 10.1029/98JA02722

Pulkkinen, A., Bernabeu, E., Thomson, A., Viljanen, A., Pirjola, R., Boteler, D., ... others (2017). Geomagnetically induced currents: Science, engineering, and applications readiness. *Space Weather*, *15*(7), 828–856.

Pulkkinen, A., & Kataoka, R. (2006). S-transform view of geomagnetically induced currents during geomagnetic superstorms. *Geophysical Research Letters*, *33*(12). Retrieved from https://agupubs.onlinelibrary.wiley.com/doi/abs/10.1029/2006GL025822 doi: 10.1029/2006GL025822

Rae, I. J., Donovan, E. F., Mann, I. R., Fenrich, F. R., Watt, C. E. J., Milling, D. K., ... Balogh, A. (2005). Evolution and characteristics of global Pc5 ULF waves during a high solar wind speed interval. *Journal of Geophysical Research: Space Physics*, *110*(A12). Retrieved from https://agupubs.onlinelibrary.wiley.com/doi/abs/10.1029/2005JA011007 doi: 10.1029/2005JA011007

Rae, I. J., Watt, C., Fenrich, F., Mann, I., Ozeke, L., & Kale, A. (2008). Energy deposition in the ionosphere through a global field line resonance. *Annales Geophysicae*, *25*(12), 2529–2539.

Russell, C. T., Luhmann, J. G., Odera, T. J., & Stuart, W. F. (1983). The rate of occurrence of dayside Pc 3,4 pulsations: The L-value dependence of the IMF cone angle effect. *Geophysical Research Letters*, *10*(8), 663-666. Retrieved from https://agupubs.onlinelibrary.wiley.com/doi/abs/10.1029/GL010i008p00663 doi: 10.1029/GL010i008p00663

Shen, X.-C., Shi, Q., Wang, B., Zhang, H., Hudson, M. K., Nishimura, Y., ... others (2018). Dayside Magnetospheric and Ionospheric Responses to a Foreshock Transient on 25 June 2008: 1. FLR Observed by Satellite and Ground-Based Magnetometers. *Journal of Geophysical Research: Space Physics*, *123*(8), 6335–6346.

Shi, X., Baker, J. B. H., Ruohoniemi, J. M., Hartinger, M. D., Murphy, K. R., Rodriguez, J. V., ... Angelopoulos, V. (2018). Long-Lasting Poloidal ULF Waves Observed by Multiple Satellites and High-Latitude SuperDARN Radars. *Journal of Geophysical Research: Space Physics*, *123*(10), 8422-8438. Retrieved from https://agupubs.onlinelibrary.wiley.com/doi/abs/10.1029/2018JA026003 doi: 10.1029/2018JA026003

Sibeck, D. G. (1990). A model for the transient magnetospheric response to sudden solar wind dynamic pressure variations. *Journal of Geophysical Research: Space Physics*, *95*(A4), 3755-3771. Retrieved from https://agupubs.onlinelibrary.wiley.com/doi/abs/10.1029/JA095iA04p03755 doi: 10.1029/JA095iA04p03755

Sibeck, D. G., Phan, T.-D., Lin, R., Lepping, R., & Szabo, A. (2002). Wind observations of foreshock cavities: A case study. *Journal of Geophysical Research: Space Physics*, *107*(A10), SMP–4.

Takahashi, K., Lee, D.-H., Merkin, V. G., Lyon, J. G., & Hartinger, M. D. (2016). On the origin of the dawn-dusk asymmetry of toroidal Pc5 waves. *Journal of Geophysical Research: Space Physics*, *121*(10), 9632-9650. Retrieved from https://agupubs.onlinelibrary.wiley.com/doi/abs/10.1002/2016JA023009 doi: 10.1002/2016JA023009

Takahashi, K., McPherron, R. L., & Terasawa, T. (1984). Dependence of the spectrum of Pc 3-4 pulsations on the interplanetary magnetic field. *Journal of Geophysical Research: Space Physics*, *89*(A5), 2770-2780. Retrieved from https://agupubs.onlinelibrary.wiley.com/doi/abs/10.1029/JA089iA05p02770 doi: 10.1029/JA089iA05p02770

Wang, B., Nishimura, Y., Hietala, H., Shen, X.-C., Shi, Q., Zhang, H., ... others (2018). Dayside Magnetospheric and Ionospheric Responses to a Foreshock Transient on 25 June 2008: 2. 2-D Evolution Based on Dayside Auroral Imaging. *Journal of Geophysical Research: Space Physics*, *123*(8), 6347–6359.

Wright, A. N., Elsden, T., & Takahashi, K. (2018). Modeling the dawn/dusk asym-

metry of field line resonances. *Journal of Geophysical Research: Space Physics*, *123*(8), 6443-6456. Retrieved from https://agupubs.onlinelibrary.wiley.com/doi/abs/10.1029/2018JA025638 doi: 10.1029/2018JA025638

Yagova, N. V., Pilipenko, V. A., Lanzerotti, L. J., Engebretson, M. J., Rodger, A. S., Lepidi, S., & Papitashvili, V. O. (2004). Two-dimensional structure of long-period pulsations at polar latitudes in Antarctica. *Journal of Geophysical Research: Space Physics*, *109*(A3). Retrieved from https://agupubs.onlinelibrary.wiley.com/doi/abs/10.1029/2003JA010166 doi: 10.1029/2003JA010166

Yumoto, K., Saito, T., Akasofu, S.-I., Tsurutani, B. T., & Smith, E. J. (1985). Propagation mechanism of daytime Pc 3-4 pulsations observed at synchronous orbit and multiple ground-based stations. *Journal of Geophysical Research: Space Physics*, *90*(A7), 6439-6450. Retrieved from https://agupubs.onlinelibrary.wiley.com/doi/abs/10.1029/JA090iA07p06439 doi: 10.1029/JA090iA07p06439

Zhang, H., Sibeck, D. G., Zong, Q.-G., Omidi, N., Turner, D., & Clausen, L. (2013). Spontaneous hot flow anomalies at quasi-parallel shocks: 1. observations. *Journal of Geophysical Research: Space Physics*, *118*(6), 3357–3363.

Zhang, X. Y., Zong, Q.-G., Wang, Y. F., Zhang, H., Xie, L., Fu, S. Y., ... Pu, Z. Y. (2010). ULF waves excited by negative/positive solar wind dynamic pressure impulses at geosynchronous orbit. *Journal of Geophysical Research: Space Physics*, *115*(A10). Retrieved from https://agupubs.onlinelibrary.wiley.com/doi/abs/10.1029/2009JA015016 doi: 10.1029/2009JA015016

Zong, Q., Rankin, R., & Zhou, X. (2017). The interaction of ultra-low-frequency Pc3-5 waves with charged particles in Earths magnetosphere. *Reviews of Modern Plasma Physics*, *1*(1), 10.